Effects of Rotor Pole Angle on Torque Characteristics of a limited-angle torque motor

Eui-Chun Lee[1], Soon-O Kwon[1], Ho-Young Lee[1], Seung-Gyo Jang[2], Jung-Pyo Hong[3]
[1]Dept. Technology Convergence Group, Korea Institute of Industrial Technology, Daegu, South Korea, 2chun@kitech.re.kr
[2] 4th R&D Institute, Agency for Defense Development, Daejeon, Korea, jsg4580@add.re.kr
[3]Dept. Automotive Engineering, Hanyang University, Seoul, Korea, hongjp@hanyang.ac.kr

***Abstract*— This paper presents a reluctance-type limited-angle torque motor (LATM), which is used for actuator or arming device in the aerospace industry, and its electromagnetic (EM) characteristics were examined with respect to changes in the rotor pole angle and the rotational position of the LATM. Among the various shape design parameters of the LATM, changes in the rotor pole angle theoretically influence the cross-sectional area of the air-gap, thereby influencing torque generation. A three-dimensional EM finite-element analysis (FEA) was used to evaluate the irregular distribution of the magnetic flux inside the LATM. Finally, an LATM model having a pole angle at which the average and maximum torque become the largest and the torque ripple becomes the smallest (20% or lower) was designed.**

Keywords*— Reluctance Motor, LATM, Limited Angle Torque Motor, Reluctance Torque, Pole Angle Effect

NOMENCLATURE

B	Flux density
Φ	Magnetic flux
V	Volume of the gap
T	Torque for rotor radius of r
r	Rotor radius
θ	Rotation position
μ_0	Permeability
l_g	Gap length
S	Cross-sectional area
R_g	Magnetic resistance of air
W_{fm}	Magnetic energy
F_x	Tangential force
W_m	Magnetic storage energy

I. INTRODUCTION

A limited-angle torque motor (LATM) is an electromagnetic (EM) actuator that rotates through a limited range of angles. It does not need a separate inverter, and the torque is generated by applying a direct-current (DC) voltage.

Reluctance-type LATMs are advantageous in high-altitude environments and extremely cold/hot environments because their performance does not significantly change with the temperature of the permanent magnet (PM) and a brush motor

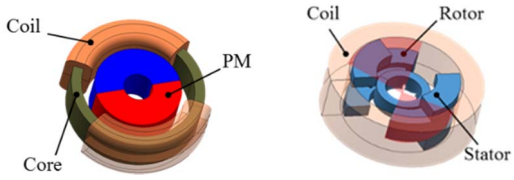

Fig.1 Structure of LATM: (A) PM Type LATM. (B) Reluctance type LATM.

(DC motor) or inverter control (a brushless DC electric motor) is not needed, in contrast to PM-type LATMs. Owing to these advantages, the reluctance LATM has a high driving safety and has been widely applied to scanners in aerospace engineering, electric drive switchgears, arming mechanisms, and so on [1]. A PM-type LATM with two poles can operate up to 180° structurally [2-3]. The structures of the two types of LATMs are shown in Fig. 1.

This paper presents a reluctance-type LATM model, as shown in Fig. 2 (A), which can operate from 0° to 90° at maximum depending on the rotor pole angle. The applications utilizing this model have an operating range of 60° or less and are designed to return to the initial position after turning off the DC power by the elastic force of a spring which is connected to rotor shaft. One of the key points in the design of the torque motor is to determine the shape of each component to determine the torque in a fixed space. In order to achieve this, calculations and verification of various forms of design elements were required and various methodologies were presented from the perspective of optimization [4].

In this study, we observed how the torque values were affected by a single variable angle. The torque characteristics were analyzed with respect to the change in the pole angle, which is expected to be the most influential factor in the generation of reluctance torque among the shape design parameters of the LATM. As shown in Fig. 2 (B), because the rotor rotates on the rotary motion of the z axis in Fig. 3 (A), specifically specifying the motion between the stator and stator, a three-dimensional (3D) magnetic-field distribution must be reflected in the torque calculation, including the fringing effect among the stators, rotors, and housing. A specific pole-angle model with larger maximum and average torques and a smaller number of torque ripples was selected through 3D EM finite element analysis (FEA). In this paper, the description of feature of the PM Type and the reluctance

978-1-5090-4281-4/17/$31.00 ©2017 IEEE

type of LATM is in the Intro section, the description of structure and operation principles of LATM is in the article II, description of numerical analysis and reluctance torque equation derived from the electromagnetic theory is in the article III, description of 3-D EM FEA results to verify the performance of LATM is in the article IV, and compare the EM simulation and measured results from the experiment of LATM is described in the article V.

II. Structure and Driving Principle of the Reluctance-Type LATM

A. Structure of the Reluctance-Type LATM

The LATM in Fig. 2 (A) consists of the stator, the rotor, the housing and the coil. The stator has four poles while the rotor has two. In the OFF state, the rotors are aligned in the initial position by the spring torque. The spring was not considered for EM performance because it was located outside the housing and would therefore not be affected by the electric-field distribution.

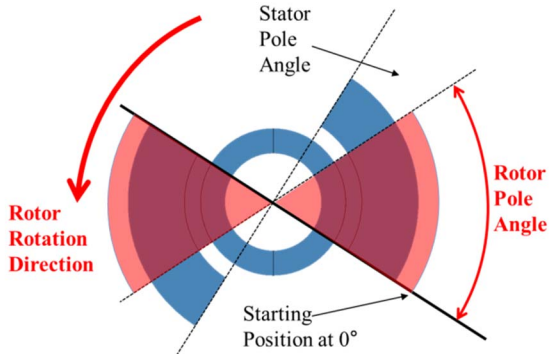

(A)

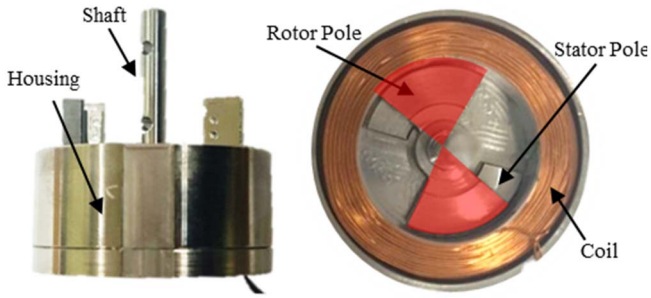

(B)

Fig. 3 (A) Starting position of the LATM. (B) Prototype of the LATM.

B. Specifications and driving principle of the reluctance-type LATM

The LATM in Fig. 2 (A) is a slot less-type motor, the coil is wound in the direction of rotation of the shaft axis. The LATM was first designed to generate a reluctance torque while suppressing the magnetic saturation of the stator, rotor, and housing within the predefined outer diameter limit. The initial position of the rotor was set in such a manner that the maximum torque section would be located in the present operating section. The flux is formed in the flux-path direction in Fig. 2 (B) to induce a change in the magnetic storage energy between the stator and the rotor with respect to the rotor position. The starting position of the LATM and photographs of a prototype of the LATM are shown in Figs. 3 (A) and (B), respectively.

TABLE I. Initial Design Specifications of Reluctance-Type LATM

Item		Units	Value
Pole Angle	***Stator Pole Angle***	***Deg.***	90
	Rotor Pole Angle		75
Spec.	***Voltage / Current***	***V/A***	28 / 1
	Armature Resistance	**Ω**	27
	Coil Diameter	***mm***	Φ 0.22
	Number of turns	***number***	500
	Average torque (0°–60°)	***gf· cm***	165.52
	Air-gap	***mm***	0.2
Material	***Stator, Rotor, Housing***	1010 Steel [Cold Rolled]	
	Coil	Copper	
	Shaft	SUS304	

III. Reluctance Torque Theory and Numerical Analysis

Some necessary explanation should be listed as follows. The reluctance torque of the reluctance-type LATM is expressed as

$$T = r \cdot F_x = \frac{\partial W_m(\theta, i)}{d\theta} \quad (1)$$

T is generated by the imbalance in the relative magnetic storage energy in the gap between the stator and the rotor and is induced in the direction that reduces the magnetic storage energy. The flux density in Fig. 2 (B) is obtained through a numerical analysis reflecting the structural geometry and electric input, and the magnetic energy W_{fm} with respect to the rotational position of the rotor is obtained from the flux density as follows:

$$W_{fm} = \frac{1}{2}\int_{vol} \frac{B^2}{\mu} dV\,[J] \quad (2)$$

The magnetic energy with respect to the position is accumulated at the location where the permeability is small. Most magnetic energy is stored in the gap because the permeability of the rotors and stators are ferromagnetic bodies. The magnetic field energy accumulated in the gap is expressed as follows:

$$W_{fm} = \frac{1}{2}\frac{B^2}{\mu_0}V = \frac{1}{2}\frac{B^2}{\mu_0}\frac{S^2 l_g}{S} = \frac{1}{2}\Phi^2\frac{l_g}{\mu_0 s} = \frac{1}{2}R_g\Phi^2\,[J] \quad (3)$$

The magnetic energy (J) and flux density (λ) of the LATM (Table 1) for pole angles in the range of 50°–80° are plotted as function of the mechanical angle in Figs. 4 (A) and (B). When the magnetic energy obtained from Eq. (3) is substituted in the general equation for the force, the following expression is obtained:

$$F = -\frac{\partial W_{fm}(\phi, x)}{\partial x} = -\frac{1}{2}\Phi^2\frac{\partial R_g}{\partial x}\,[N] \quad (4)$$

Equations (2) and (3) can be used to predict the changing characteristics of the linkage magnetic flux and inductance with respect to the rotation angle of the LATM rotor. On the basis of Eq. (4), the reluctance force is generated in the direction that minimizes the magnetic resistance, and the torque is generated in the rotation direction around the Z axis that maximizes the cross-sectional area of the gap.

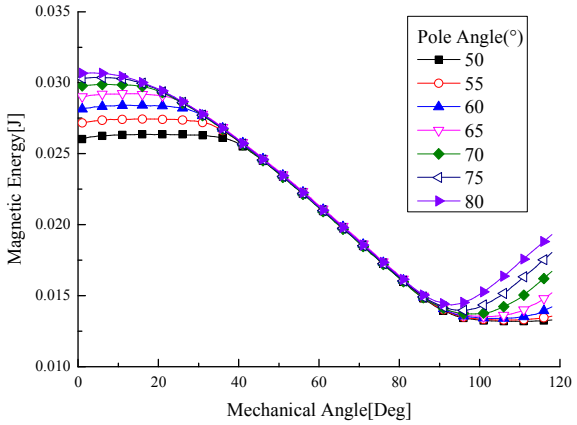

(A)

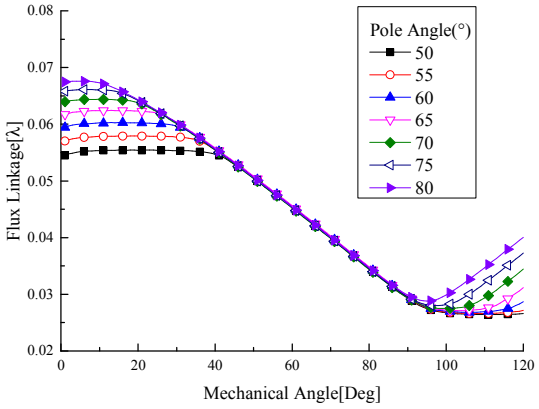

(B)

Fig. 4 Electromagnetic characteristics with respect to the mechanical angle for rotor pole angles in the range of 50°–80°. (A) Magnetic energy of each model and (B) flux linkage of each model.

IV. Evaluation of the Electromagnetic Performance of the LATM using FEA

A. 3D EM FEA of the reluctance-type LATM

The LATM models in Table 2 were created with the initial design specifications in Table 1 by changing the rotor pole angle in the range of 50°–80° as the design variable. FEA is performed using a commercial electromagnetic field simulation software, Infolitica MagNet (V7.7). According to the data in Table 2, the rate of change of the cross-sectional area of the air-gap with decreasing rotor pole angle is mainly based on Eq. (3), confirming the observed increasing trend of the torque.

TABLE II. |B| Distribution in the LATM for Pole Angles in the Range of 50°-80°

Pole Angle [Deg.]	**50**	**60**
|B| Distribution [T]	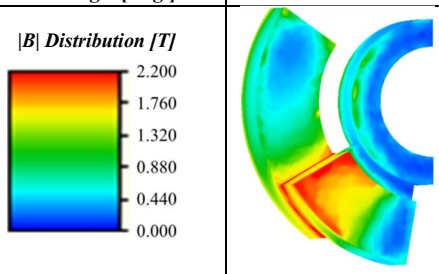	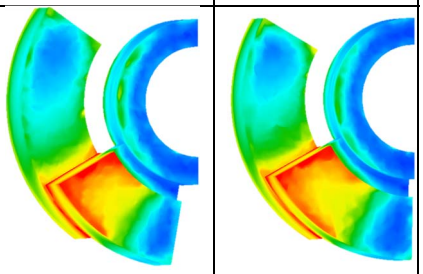
| B | Max [T]	2.408	2.365
Moving Angle [Deg.]	65	60
Torque [gf·cm]	164.66	163.40

Pole Angle [Deg.]	**70**	**80**
|B| Distribution [T]	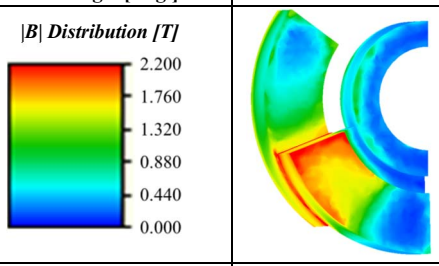	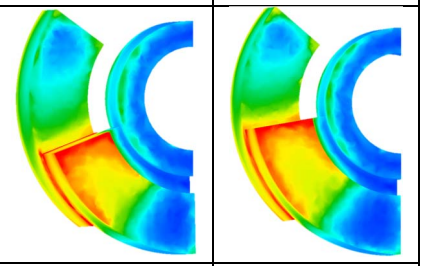
| B | Max [T]	2.581	2.430
Moving Angle [Deg.]	55	50
Torque [gf · cm]	159.19	152.99

B. Torque characteristics of the LATM

Fig. 3 (A) and (B) show that the absolute value of the rotor pole angle of the LATM tends to coincide with the absolute value of the rotor rotation range that includes a flat torque section. Thus, for this LATM with an operating range of 60°, the rotor pole angle needs to be designed to be greater than 60° at minimum. The torque ripple in Fig. 5 (B) is defined by

$$T_{RF} = \frac{\Delta T_{pp}}{T_{av}} \quad (5)$$

where ΔT_{pp} is the peak value of the torque and T_{av} is the average torque.

Fig. 5(A) shows the torque with respect to the moving angle of the rotor for models with pole angles in the range of

50°–80°. Among the analysis models in Fig. 5 (B), the model with a pole angle of 65°, which has the highest maximum and average torques and a torque ripple less than 20%, was found to have suitable specifications for application to the system. Furthermore, the change in the average torque was greater than the change in the maximum torque for changes in the pole angle of the LATM.

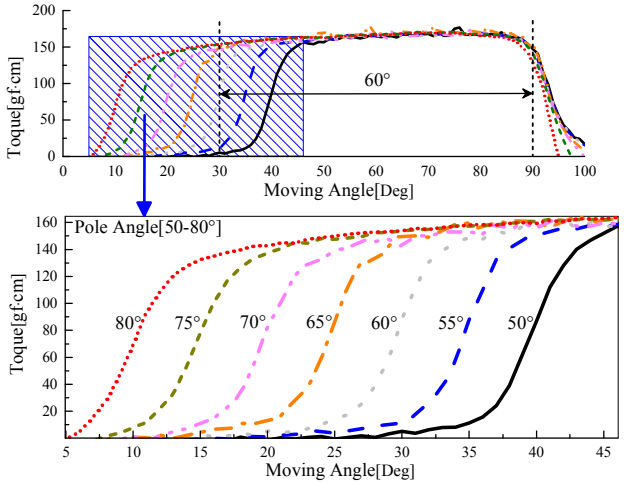

(A)

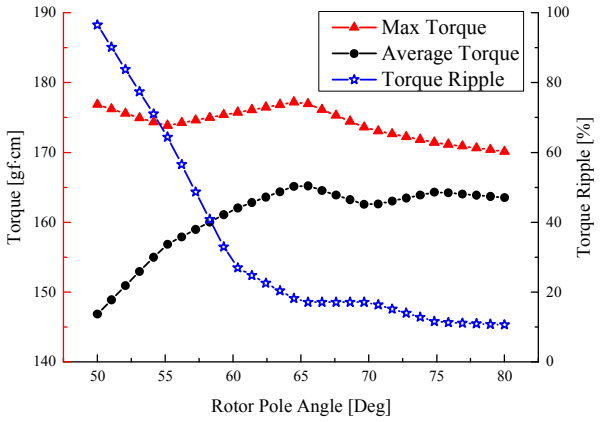

(B)

Fig. 5 (A) Torque with respect to the rotation moving angle of the rotor for models with pole angles in the range of 50°–80°. (B) Maximum torque, average torque, and torque ripple for the same models.

C. *Target specification model analysis (pole angle 65° LATM)*

In Fig. 5 (B), the model with a pole angle of 65° was selected as it maximizes the maximum and average torques and maintains the torque ripple within 20% according to the system requirements. Moreover, the rotational torque and the normal force with respect to the rotation angle were measured through FEA, as shown in Fig. 5(A) and Fig. 6, respectively. Furthermore, after confirming the distributions of the magnetic flux density and the maximum magnetic flux density (Max B) of the rotor according the rotation angle of LATM, as summarized in Table 3, it was verified that the maximum magnetic flux density tended to increase as the areas of the facing sections of the stator and the rotor increased when they rotated about the Z axis. As shown in Equation (3), the torque generated by the operation of LATM and the air-gap flux density tends to increase as the amount of variation of the air-gap cross section increases.

TABLE III. |B| DISTRIBUTION WITH RESPECT TO THE MOVING ANGLE OF THE MODEL WITH A POLE ANGLE OF 65°

Relative Position [Deg.]	0	10
|B| Distribution [T] 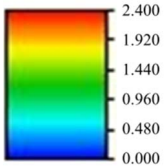	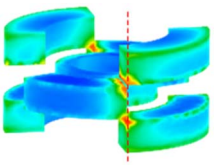	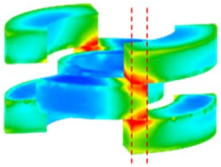
|B| Max [T]	2.377	2.378
Torque [gf·cm]	147.78	169.63

Relative Position[Deg.]	20	30
|B| Distribution [T] 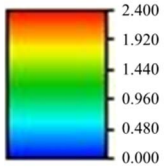	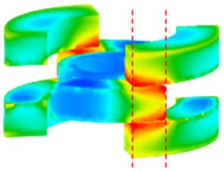	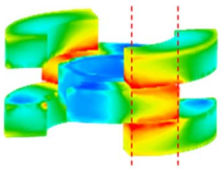
|B| Max [T]	2.471	2.482
Torque [gf· cm]	170.65	164.32

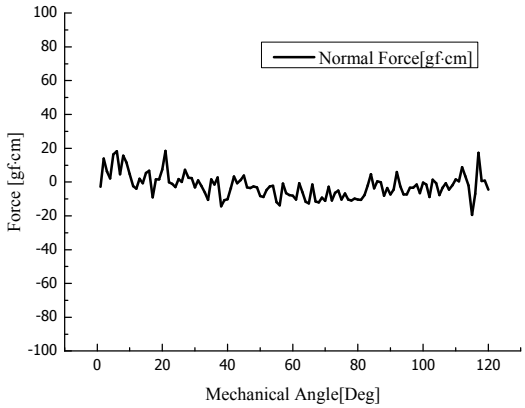

Fig. 6 Normal force of the LATM with a pole angle of 65°.

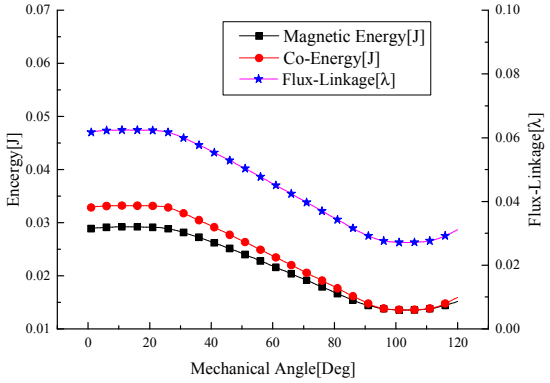

Fig. 7 Co-energy, magnetic energy, and flux linkage of the LATM with a pole angle of 65°.

Therefore, a relatively high torque is generated starting from a mechanical moving angle of 20°, at which the rotor and stator approach each other. In Table 3, the rate of torque increase is relatively small since the variation of the air-gap cross-sectional area is constant beyond a moving angle 20°.

D. Manufacturing tolerance evaluation of the LATM

The evaluation process of electrical/mechanical manufacturing tolerance of the LATM is presented in Fig. 8.

- First, the FEA-calculated inductance value obtained from the constructed core model of the LATM is compared to the inductance value measured with an LCR meter. For instance, the measured inductance value of Fig. 4 (B) is less than the FEA-calculated value. This result indicates that the air-gap of the LATM model is larger than that of the initial design or the number of windings is less than that of the initial design, if the electric input is correct.
- Second, the measured torque is compared to the FEA-calculated torque value obtained from the constructed structure of the LATM. For instance, if the measured torque is less than the calculated torque (FEA), this result indicates that the tolerance of air-gap clearance of the LATM model is larger than that of the initial design or that mechanical friction exists because of the eccentricity of the rotor and shaft of the LATM.

The windings (number of turns), imbalance of air-gap tolerance, mechanical friction from manufacturing, and assembly accumulative air-gap of the LATM are examined separately to determine the LATM manufacturing tolerance. Through the process shown in Fig. 8, if the performance of the manufactured LATM does not meet the criteria, the defects during the manufacturing of the LATM can be determined to give feedback to the production stage of the LATM.

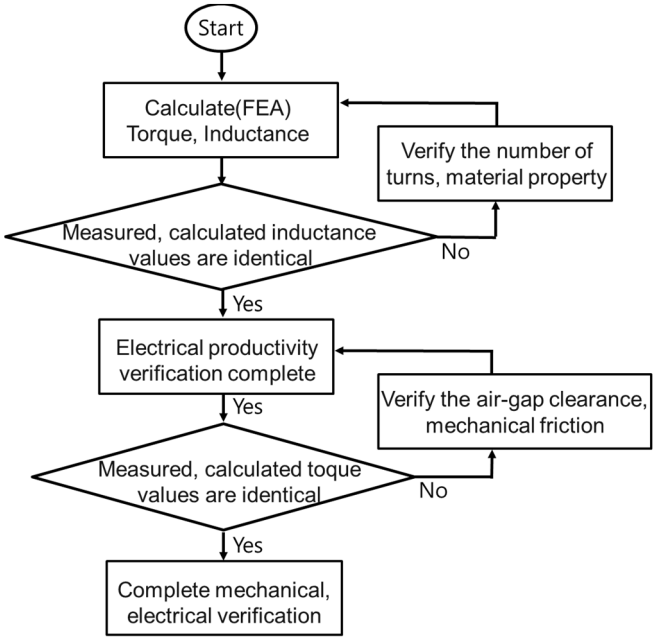

Fig. 8 Manufacturing tolerance evaluation process of the LATM.

V. RESULTS

Figs. 9 (A)-(C) show each part of the model with a pole angle of 65° constructed by changing the pole angle to 65° in the initial design specifications of Table 1. A cogging torque measuring instrument was used to investigate different torque characteristics at the LATM rotation angle shown in Fig. 10. Specific experimental conditions were set according to Table 1. In particular, the current input affecting the LATM magneto motive force (MMF) was set to be 1 A. As shown in Fig. 10, the experimentally measured torque and the torque value calculated using 3D FEA show a difference of approximately 15%. This error is mainly attributed to an increase of friction force on the shaft-axis bearing due to the axial normal force shown in Fig. 6 or the change of air-gap length with the accumulated machining errors. In this LATM model, the air-gap length is 0.2 mm, which is very small compared to the air-gap design of a general PM-type motor. Therefore, there is a relatively large change in the torque characteristics with respect to the change of air-gap length of the LATM.

(A) Housing (lower stator) and coil wound

(B) Rotor and shaft

(C) Housing (upper stator)

(D) Torque meter and LATM

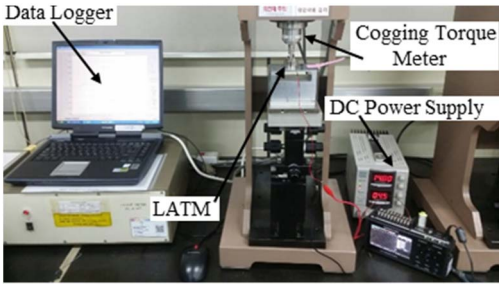

(D) Experiment setup (KETI, S. Korea)

Fig. 9 Experimental LATM model with a pole angle 65° (A-D).

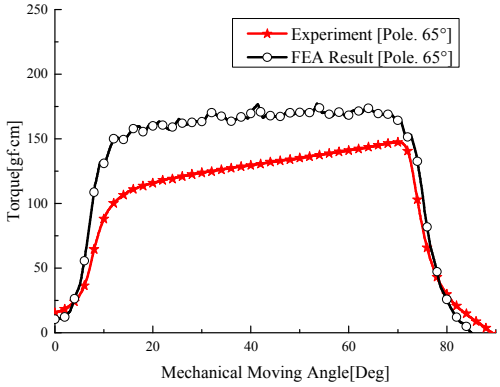

Fig. 10 Experiment result and 3D FEA result for the LATM model with a pole angle of 65°.

VI. Conclusion

The torque characteristics of a reluctance-type LATM were investigated with respect to changes in the rotor pole angle. The range of average torque tended to widen as the pole angle increased, whereas the maximum torque tended to decrease. Thus, the model having a pole angle of 65° was selected because it shows the maximum torque and a small torque ripple (less than 20%). In particular, the initial design of the reluctance-type LATM was more advantageous if the rotor pole angle is larger than the minimum rotor rotation angle. The results were experimentally tested using a prototype LATM with a pole angle of 65°.

In addition to the pole angle, further research on the torque characteristics with respect to changes in the shapes of the structures that can influence the magnetic-field distribution in the proposed design is needed. Furthermore, in the case of an LATM that continuously repeats rotational motions, the thermal characteristics should be analyzed with respect to the magnetic saturation.

ACKNOWLEDGEMENT

Special thanks to Infolytica MagNet (V7.7) electromagnetic simulation software and LC-TEK Co., Ltd.

REFERENCES

[1] S.-O. Kwon et al., “Study on the characteristic analysis of limited angle torque motor,” KIEE, July 2014.

[2] M. Krishna et al., “Brushless DC limited angle torque motor,” Proceedings of the International Conference on Power Electronics, Drives and Energy Systems for Industrial Growth, Jan. 1996.

[3] P. Hekmati, et al., “Design and analysis of a novel axial flux slotless limited angle torque motor with trapezoidal cross section for the stator,” IEEE Trans. Energy Conv., vol. 28, No. 4, December 2013.

[4] T. T. Overboom ,et al. Design and Optimization of a Rotary Actuator for a Two-Degree-of-Freedom zφ-Module, IEEE TRANSACTIONS ON INDUSTRY APPLICATIONS, VOL. 46, NO. 6, NOVEMBER/ DECEMBER 2010

[5] J.-M. Kim et al., “Analysis of cogging torque caused by manufacturing tolerances of surface mounted permanent magnet synchronous motor for electric power steering,” IET Electric. Power Appl., vol. 10(8), pp. 691–696, 2016.

[6] P. Hubler and M. Poschell, “Actuators for steam and process engineering,” Sulzer Tech. Rev., vol. 4, pp. 228-232, 1974.

[7] D. Taylor, “Electric actuators,” Control & Instrwn., vol. 2, pp. 25-29, 1970.

[8] A. S. Conner, “Positional control rotary actuator,” CEGB Technical.

[9] I. Chang, “How to choose a rotary actuator,” Hydraul. & Pneu., vol. 29, pp. 66-69, 1976.

[10] H. Fuller, “Electric valve actuation,” Instrum. Control Syst., vol. 49, pp. 29-32, 1976.

[11] A. Anderson, “Controlling fluid flow electrically,” Machine Des., vol. 46, pp. 112-117, 1974.